Water Soluble Photo- and Electroluminescent Alkoxy-Sulfonated Poly(*p*-phenylenes) Synthesized via Palladium Catalysis

Seungho Kim, Jennifer Jackiw, Edward Robinson, Kirk S. Schanze, and John R. Reynolds*

Department of Chemistry, Center for Macromolecular Science and Engineering, University of Florida, Gainesville, Florida 32611

Jeff Baur and Michael F. Rubner

Department of Materials Science, Massachusetts Institute of Technology, Cambridge, Massachusetts 02139

Danielle Boils

Xerox Research Centre of Canada Mississauga, Ontario, Canada L5K 2L1

Received June 3, 1997; Revised Manuscript Received November 21, 1997

ABSTRACT: Water soluble poly(*p*-phenylene) derivatives, poly[2,5-bis(3-sulfonatopropoxy)-1,4-phenylene-*alt*-1,4-phenylene] sodium salt (PPP−$OPSO_3$) and poly[2,5-bis(3-sulfonatopropoxy)-1,4-phenylene-*alt*-4,4′-biphenylene] sodium salt (PPBP−$OPSO_3$), have been synthesized through a Suzuki coupling reaction of 1,4-dibromo-2,5-bis(3-sulfonatopropoxy)benzene sodium salt with 1,4-phenylenediboronic acid or 4,4′-biphenyldiyldiboronic acid 2,2′-dimethylpropyl diester using a water soluble Pd(0) catalyst or $Pd(OAc)_2$. The pH dependence of the coupling reaction was investigated and resulted in pH independence at pH levels greater than 10.0. End group analysis of PPP−$OPSO_3$ via ^{1}H NMR of *tert*-butyl end-capped polymers indicates degrees of polymerization in excess of 40 (ca. 80 rings per chain). Viscometric analysis of PPP−$OPSO_3$ in water shows a behavior comparable to sodium poly(styrenesulfonate) (PSS) of molecular weight 8000. In addition, the polyelectrolyte effect is observed at low polymer concentrations. The λ_{max} of the $\pi \rightarrow \pi^*$ absorption for PPP−$OPSO_3$ is found at 339−342 nm, while that of PPBP−$OPSO_3$ shows a bathochromic shift to 349−352 nm. All of the water soluble PPP oligomers and polymers feature strong blue fluorescence. The fluorescence has been characterized by quantum yield and lifetime studies. Nanosecond−microsecond laser flash photolysis experiments indicate that direct excitation of the polymers in the near-UV leads to triplet state formation, albeit with comparatively low efficiency. Multilayered films of PPP−$OPSO_3$ were fabricated with poly(ethyleneimine) (PEI) using layer-by-layer self-assembly and incorporated into blue-light-emitting devices.

Introduction

Pendant group functionalization of conjugated polymers has proven to be a useful method for improving the processability of these typically insoluble and infusible materials. In the case of unsubstituted poly(*p*-phenylene) (PPP) prepared under mild conditions via the reaction between dihaloaromatic compounds and Mg metal in the presence of various low-valent Ni catalysts, fully 1,4-linked polymers precipitate from the reaction medium at $X_n = 5-10$.[1] While high molecular weight polyphenylenes were prepared via soluble precursor methodologies, approximately 15% of the repeat units are 1,2-linked, preventing the formation of a fully conjugated and rigid rod polymer upon elimination.[2,3] These problems were subsequently circumvented by Grubbs et al. by the bis[(allyl)(trifluoroacetato)nickel-(II)]-initiated polymerization of cyclohexadiene derivatives to produce 100% 1,4-linked polycyclohexenes that could be efficiently converted to PPP.[4] To prepare soluble PPP's, Schlüter and Wegner utilized Yamamoto and Suzuki coupling conditions to polymerize alkyl-derivatized benzenes.[5] By judicious choice of catalyst and polymerization conditions, they were able to prepare soluble polymers with X_n of approximately 50. Further synthetic research in this field has been directed toward preparing PPP derivatives and related aromatic polymers with functional groups attached to, or incorporated within, the backbone. For example, Kim and Webster[6] synthesized a trifunctional benzene-based monomer, (3,5-dibromophenyl)boronic acid, which could be self-condensed to a hyperbranched macromolecule that is water soluble. Novak et al.[7] subsequently reported the synthesis of a water soluble, rigid rod PPP derivative using a water soluble Pd(0) catalyst. This PPP derivative contains two carboxylic acid groups directly attached to each quaterphenylene repeat unit and all *para* linkages along its backbone. Subsequently, Rehahn et al.[8] prepared a series of PPP-based polyelectrolytes containing both carboxylate and tetralkylammonium functionality, while Wegner et al.[9a] prepared directly sulfonated PPP's via an organic soluble precursor. These were later used in the formation of blue-light-emitting devices.[9b]

Since the discovery that PPP's could be converted to a highly conducting form upon oxidative doping, the optoelectronic properties of this class of fully conjugated polymers have been of intense interest.[9] In the neutral form, polyphenylenes are highly luminescent and have been successfully used as the active emitting material in LED's, giving a strong blue color.[10]

With the background given above, we targeted the synthesis of a new type of water soluble PPP based on the utilization of sulfonatopropoxy groups.[11] We have found this pendant group to be versatile in its ability

S0024-9297(97)00781-X CCC: $15.00
Published on Web 01/27/1998

to induce water solubility into a number of aromatic polymers.[12−14] In the case of PPP, positioning the alkoxy oxygen directly attached to the main chain provides a small steric barrier to planarity. In addition, the electron-donating nature of the propoxy linkage serves to lower the oxidation potential, leading to enhanced charge carrier stability over other substituted PPP's.

Two polymers, specifically, poly[2,5-bis(3-sulfonatopropoxy)-1,4-phenylene-*alt*-1,4-phenylene] sodium salt (PPP−$OPSO_3$, **1**) and poly[2,5-bis(3-sulfonatopropoxy)-1,4-phenylene-*alt*-4,4′-biphenylene] sodium salt (PPBP−$OPSO_3$, **2**), have been the focus of this work.

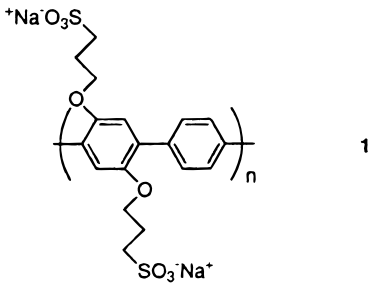

1

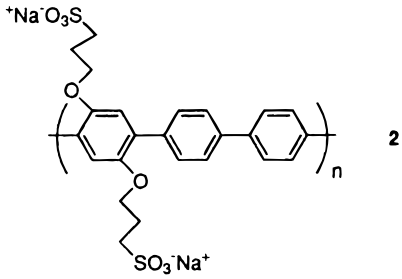

2

The water soluble Pd(0) catalyst, Pd[$P(C_6H_5)_2C_6H_4$-*m*-$SO_3^-Na^+]_3$ was initially used for the syntheses of PPP−$OPSO_3$, which contains a biphenyl repeat unit, and PPBP−$OPSO_3$, which contains a terphenyl repeat unit. On the basis of the work of Novak et al.,[15] who reported on the catalytic activity of air stable $Pd(OAc)_2$, we have also used this catalyst in our polymerizations. We have studied the structure of these polymers by a combination of ^{13}C NMR, ^1H NMR (including end group analysis), FT-IR, UV−vis, viscometry, and solution fluorescence. As these polymers are fluorescent, they have been incorporated into electroluminescent devices using a layer-by-layer sequential adsorption process. In this manner, diodes have been constructed that emit blue light.

Results and Discussion

Monomer Syntheses. To carry out effective polymerizations, we have found that 1,4-phenylenediboronic acid (**3**) can be sufficiently purified for use in step-growth polymerization chemistry. On the other hand, to insert an unsubstituted biphenyl into the repeat unit, we found it necessary to convert the 4,4′-biphenyldiyldiboronic acid to a diester derivative, specifically 4,4′-biphenyldiyldiboronic acid 2,2′-dimethylpropyl diester (**4**), as the acid could not be sufficiently purified by recrystallization. 1,4-Dibromo-2,5-bis(3-sulfonatopropoxy)benzene disodium salt (**5**) was synthesized according to the procedure developed in our group.[11]

Catalysts. A water soluble Pd(0) catalyst, (Pd-[$P(C_6H_5)_2C_6H_4$-*m*-$SO_3Na]_3$) (**6**) was used in the initial phase of this work but was found to be more air-sensitive than other common Pd(0) complexes such as tetrakis(triphenylphosphine)palladium. During the course of this work, coupling reactions using the air and light stable $Pd(OAc)_2$ (**7**) were reported to be faster than the Pd(0) catalyst as the triphenylphosphine groups in the Pd(0) catalyst are proposed to retard the coupling reaction.[15,16] At the same time, $Pd(OAc)_2$ is less soluble in water, motivating us to compare catalytic activity in this work. Conventional Suzuki catalysts were not employed due to their water insolubility, which would greatly retard, or completely inhibit, polymerization.

Scheme 1

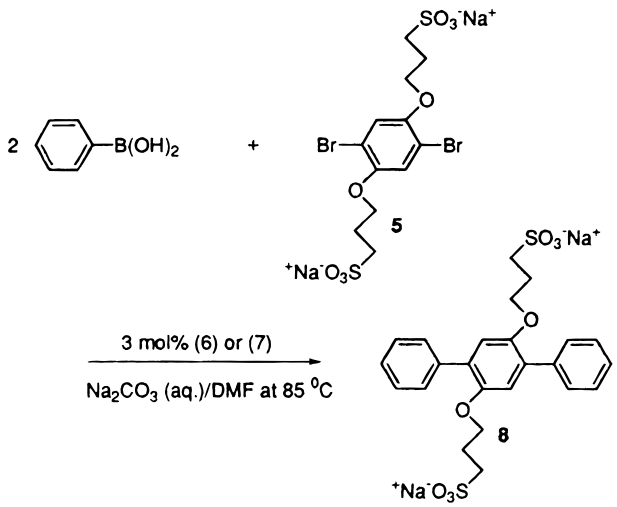

Model Compound. 2,5-Diphenyl-1,4-(2-sulfonatopropoxy)benzene sodium salt (**8**) was synthesized as both a structural model and to study the coupling reaction between the water soluble phenylboronic acid and dibromide monomers with both catalysts, as shown in Scheme 1. As used for the polymerizations, a deaerated mixture of 70% aqueous 0.2 M Na_2CO_3 with 30% DMF was used as solvent and the reaction was carried out at 85 °C under argon.

The structure of the terphenyl model **8** was characterized using ^1H and ^{13}C NMR, along with FTIR, UV−vis and elemental analysis. The NMR and elemental analysis results are as expected and are detailed in the Experimental Section. It should be noted that the moderate yields are after careful purification and are not indicative of a low-conversion reaction. The FT-IR spectrum of **8** exhibited two strong absorption bands, indicating asymmetric and symmetric S=O stretching of the sulfonate group at 1205 and 1047 cm^{-1}. In addition, aliphatic C−H stretching due to the propyl group was found at 2952 and 2874 cm^{-1}, while the aromatic C=C stretching of the benzene ring was found at 1635−1655 cm^{-1} and the aromatic C−H of the benzene ring at 3033 cm^{-1}.

The $\pi-\pi^*$ absorption of **8** in aqueous solution was observed at $\lambda_{max} = 305$ nm (4.1 eV), which is red shifted relative to the value of 276 nm (4.5 eV) for unsubstituted terphenyl.[17] While steric interactions of the sulfonatopropoxy substituents would force **8** to be less planar and lead to a blue shift in the absorption, this is compensated by the electron-donating alkoxy substituents. This result is of consequence when considering polymer spectra and the extent of conjugation, as will be discussed in detail below.

Polymer Syntheses. The polymerizations were carried out as illustrated in Scheme 2. Mixtures of 70%

Scheme 2

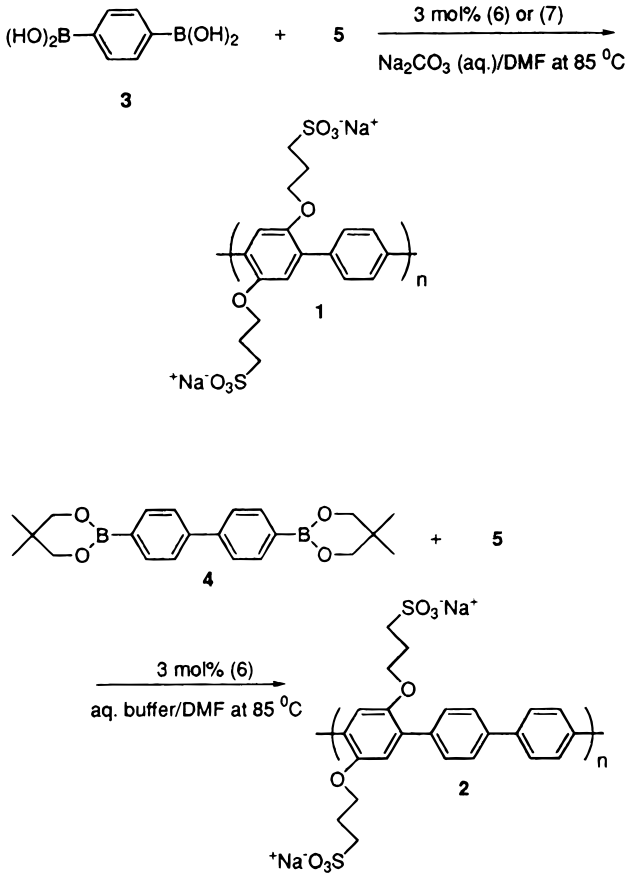

aqueous base at pH 8.0, 10.0, and 12.0 with 30% DMF were utilized as polymerization media. This solvent combination was initially used for the water soluble dicarboxy-substituted PPP synthesized by Wallow and Novak, because slightly basic conditions (ca. pH 7−8) were believed to prevent aryl exchange products, which cause defects in the rigid rod structure.[7] However, sufficient basicity for the hydrolysis step is important for increasing the solubility of the boronic acid monomer for the coupling reaction. The solution pH also has a strong effect on the polymerization rate when a diboronic ester monomer such as **4** is used. Finally, catalytic activity that may affect overall yields and molecular weight may be pH dependent. For these reasons, the pH dependence of the polymerization was studied in order to attain homogeneous and reliable reaction conditions to obtain high molecular weight polymer.

The syntheses of a series of PPP−$OPSO_3$ (**1**) polymers were carried out using the reaction conditions outlined in the Experimental Section. Typically, reactions were conducted at 85−90 °C for 24 h regardless of which catalyst was used. As the polymer remained in solution, the precipitated Pd particles were easily removed by filtration using a medium glass filter. The water soluble Pd(0) catalyst was used exclusively in the syntheses of PPBP−$OPSO_3$ (**2**) because the diboronate ester monomer (**4**) was insoluble in the aqueous buffer solvent mixture in the initial stages of the coupling reaction. In this instance, the monomer slowly dissolved into the polymerization medium as it hydrolyzed. As such, an overall slow polymerization rate was desired and we expected could be better controlled by the catalyst with a lower activity.

The catalytic activities of the two different Pd catalysts were qualitatively compared by monitoring fluorescence of the reaction under a UV lamp. As the chain length begins to build up, the nonfluorescent monomers are converted into highly fluorescent species. In all instances, the reactions using $Pd(OAc)_2$ were found to be significantly faster than those using the water soluble Pd(0) catalyst. After removal of the Pd particles by filtration, the tan-violet filtrate was dialyzed using a 3500 molecular weight cutoff membrane to remove ionic impurities and low molecular weight oligomers. The products were isolated by evaporation of the water, yielding water soluble polymers in good yields of 40−50%.

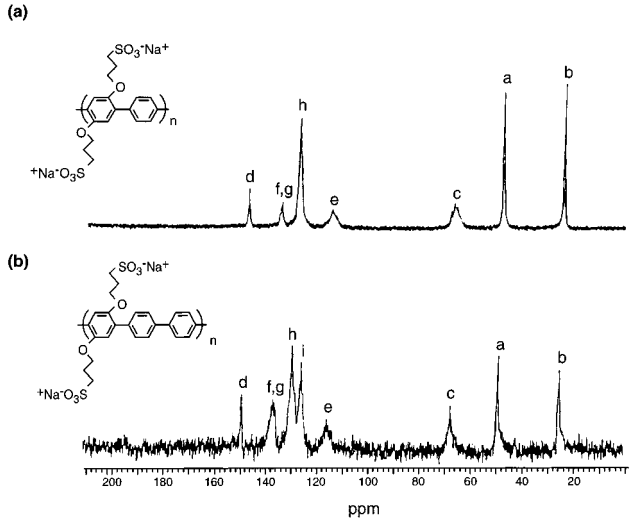

Figure 1. ^{13}C NMR spectra of (a) PPP−$OPSO_3$ and (b) PPBP−$OPSO_3$.

Polymer Structure Analysis. The molecular structures of the polymers were characterized using ^1H and ^{13}C NMR, FTIR, and elemental analysis, and the results are all consistent with the 1,4-linked polymers derivatized, which are partially hydrated, as expected. This is illustrated by the ^{13}C NMR spectra of PPP−$OPSO_3$ and PPBP−$OPSO_3$ shown in Figure 1, which shows each carbon peak clearly with its assignment. The presence of a strong peak near 137 ppm (peaks f and g) is indicative of the aryl−aryl bond formation during polymerization. The peaks near 126−130 ppm (peak h in Figure 1a, peaks h and i in Figure 1b) are assigned to the proton-containing carbons of the unsubstituted phenylene ring. The phenylene carbons bonded to the propoxy side chains are found downfield near 150 ppm (peak d). The three aliphatic carbons of the propoxy side chain are observed at 25.4, 48.9, and 68.1 ppm (peaks a, b, and c). The ^1H NMR spectra are in agreement, exhibiting three different peaks for the aliphatic hydrogens, indicating that the polymers carry two sulfonatopropoxy groups per repeat unit. Quantitative comparison of the aromatic protons assigned to the functionalized and unfunctionalized phenylene rings shows a 2:1 and a 4:1 ratio for the resonances for PPP−$OPSO_3$ and PPBP−$OPSO_3$, as expected in the high molecular weight polymer limit.

The FT-IR spectra of PPP−$OPSO_3$ and PPBP−$OPSO_3$ are quite similar, as shown in Figure 2, and are consistent with the expected structures. Two strong absorption bands are observed at 1185−1210 and 1040−1050 cm^{-1} and are assigned to the asymmetric and symmetric S=O stretching of the sulfonate groups, respectively. The aliphatic C−H stretching vibrations due to the sulfonatopropoxy groups are seen at 2935−

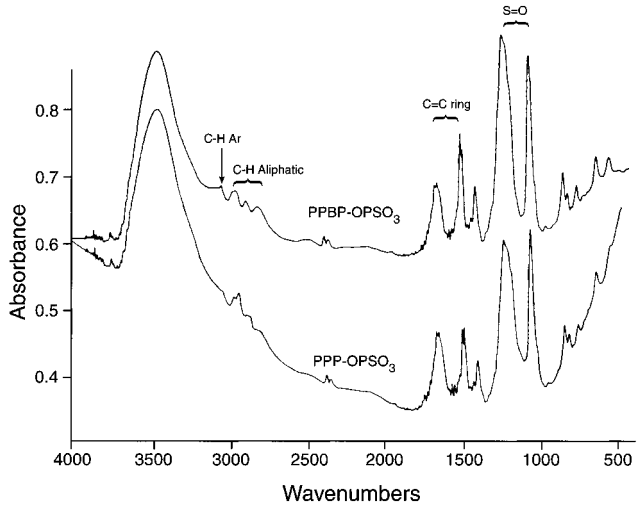

Figure 2. FT-IR spectra of (a) PPP−$OPSO_3$ and (b) PPBP−$OPSO_3$.

Table 1. Thermal Stability and UV−vis λ_{max} for PPP−$OPSO_3$ and PPBP−$OPSO_3$ Prepared as a Function of pH

polymer samples	Pd catalyst	pH of aqueous buffer	onset dec temp (°C)	λ_{max} (nm) of $\pi-\pi^*$ absorption
PPP−$OPSO_3$ (**1a**)	Pd(0) complex	8.0	354	339
PPP−$OPSO_3$ (**1b**)	Pd(0) complex	10.0	306	339
PPP−$OPSO_3$ (**1c**)	Pd(0) complex	12.0	358	342
PPP−$OPSO_3$ (**1d**)	$Pd(OAc)_2$	8.0	338	329
PPP−$OPSO_3$ (**1e**)	$Pd(OAc)_2$	10.0	360	341
PPP−$OPSO_3$ (**1f**)	$Pd(OAc)_2$	12.0	360	339
PPBP−$OPSO_3$ (**2a**)	Pd(0) complex	8.0		
PPBP−$OPSO_3$ (**2b**)	Pd(0) complex	10.0	378	352
PPBP−$OPSO_3$ (**2c**)	Pd(0) complex	12.0	301	349

2940, 2875−2880, and 2800−2805 cm^{-1}, the aromatic C=C stretch of the phenylene rings are found at 1635−1645 cm^{-1}, and the aromatic C−H stretch is found at 3030−3040 cm^{-1}. There is a close correlation of these results with those of the model compound presented earlier.

Thermal Stability. Thermogravimetric analysis results for PPP−$OPSO_3$ and PPBP−$OPSO_3$ synthesized under various conditions were carried out, and the results are summarized in Table 1. These results indicate that all of the polymers are stable to weight loss up to temperatures of 300−350 °C in nitrogen. A rapid weight loss of 20−30% occurs after the onset of decomposition and is likely due to the loss of the sulfonate and propyl functionality.

Molecular Weight Analyses. An important, yet difficult, question to answer concerning rigid rod and conjugated polyelectrolytes are their molecular weights. Wallow and Novak reported an approximate M_w of 50 000 for poly(*p*-quaterphenylene-2,2′-dicarboxylic acid), synthesized under conditions similar to those used in this work, using polyacrylamide gel electrophoresis and a single-stranded DNA molecular weight standard.[7b] They note that the method does not likely give an accurate molecular weight, since the polyphenylene polyelectrolyte is more rigid than the DNA reference.

Scheme 3

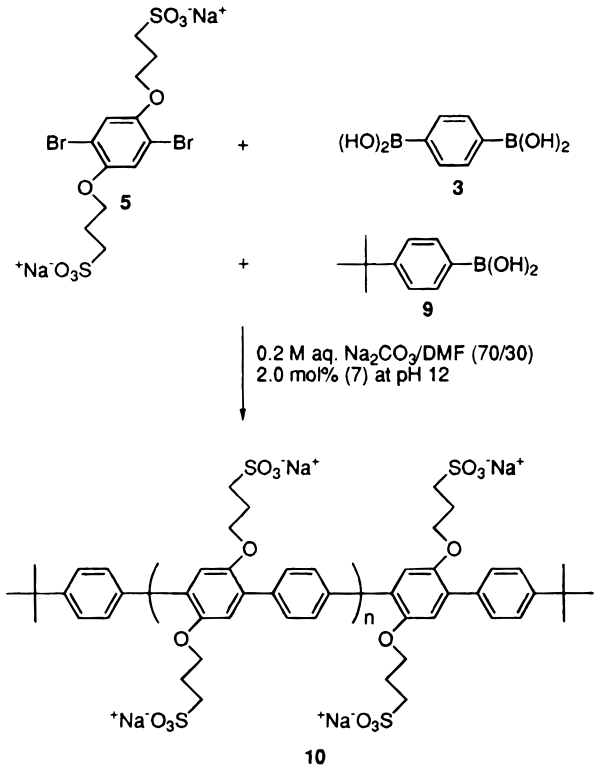

For PPP−$OPSO_3$ and PPBP−SO_3, colligative methodologies and light scattering are difficult due to their electrolyte and fluorescent nature. GPC studies were attempted using an aqueous mobile phase, but in all cases adsorption of the polymers to the columns occurred, negating the results. Matrix-assisted laser desorption/ionization-mass spectroscopy (MALDI-MS) was attempted, but the results also proved inconclusive.

To approximate the number average chain lengths, end group analysis was carried out by synthesizing polymers with a controlled amount of monofunctional boronic acid. Specifically, (4-*tert*-butylphenyl)boronic acid (**9**) was used as an end-capping reagent to produce 4-*tert*-butylphenyl-end-capped PPP−$OPSO_3$ oligomers and polymers (**10**) (TBPPP−$OPSO_3$), as shown in Scheme 3, which could then be quantitatively analyzed by ^1H NMR relative to the methylene resonances from the sulfonatopropoxy side chains. Polymerizations were run under the same reaction conditions used for the syntheses of PPP−$OPSO_3$, which, under statistically controlled step-growth polymerization conditions, would yield X_n ranging from 3−50 (6−100 phenylene rings per chain). As the Suzuki coupling used in the polymerization is not an equilibrium reaction, and since the polymers were dialyzed to remove low molecular weight ionic impurities, quantitative comparison with theoretical values of X_n was not expected but could serve as a target. In the synthesis of the lower molecular weight oligomers, a dialysis membrane with a molecular weight cutoff of 500 was employed to avoid loss of the majority of the product.

The experimentally determined X_n values are compared with the theoretical targets in Table 2 along with the λ_{max} values of the TBPPP−$OPSO_3$ long-wavelength absorption. These values can be used as a standard to predict the minimum degree of polymerization for PPP−$OPSO_3$ and demonstrate this method to be a plausible approach to molecular weight determination. Using

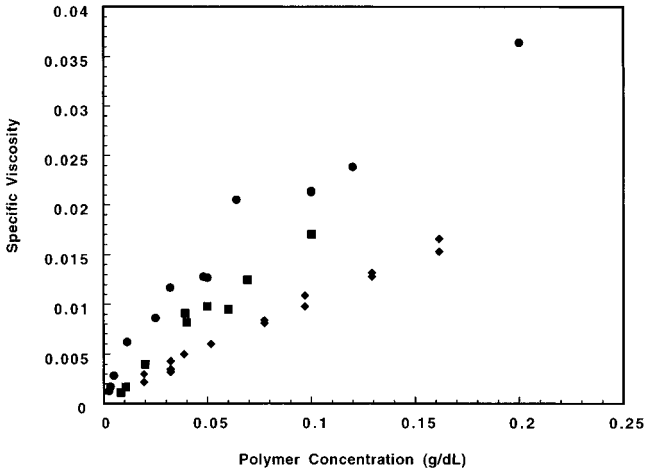

Figure 3. Specific viscosity as a function of polymer concentration for different ionic strengths: (●) PPP−OSO_3 in water; (■) PPP−OSO_3 in 0.001 M $NaNO_3$; (◆) PPP−OSO_3 in 0.1 M $NaNO_3$.

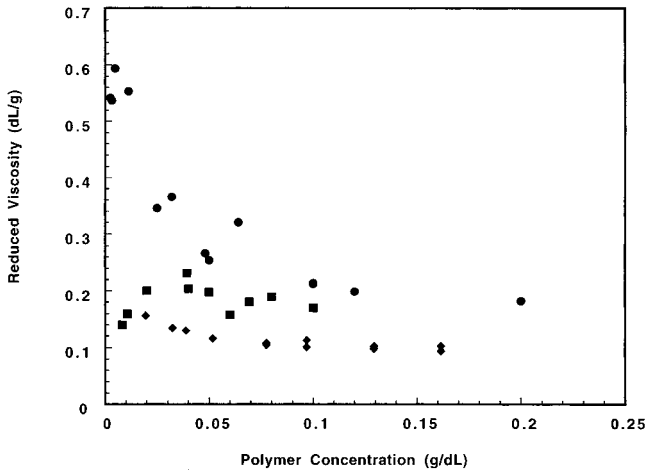

Figure 4. Reduced viscosity as a function of polymer concentration for different ionic strengths: (●) PPP−OSO_3 in water; (■) PPP−OSO_3 in 0.001 M $NaNO_3$; (◆) PPP−OSO_3 in 0.1 M $NaNO_3$.

Table 2. End-Capping Degree of Polymerization Results for TBPPP−$OPSO_3$.

polymer samples	theoretical X_n	exp X_n	λ_{max} (nm) of $\pi-\pi^*$ absorption
TBPPP−$OPSO_3$ (**10a**)	3.0	4.0	323
TBPPP−$OPSO_3$ (**10b**)	6.0	7.4	329
TBPPP−$OPSO_3$ (**10c**)	9.0	7.7	330
TBPPP−$OPSO_3$ (**10d**)	12.0	12.4	330
TBPPP−$OPSO_3$ (**10e**)	17.0	17.1	333
TBPPP−$OPSO_3$ (**10f**)	23.0	17.5	333
TBPPP−$OPSO_3$ (**10g**)	35.0	32.2	336
TBPPP−$OPSO_3$ (**10h**)	50.0	41.9	338

these results, and the fact that the λ_{max} values of the PPP−$OPSO_3$ long-wavelength absorption ranged from 339 to 342 nm, suggests that the X_n is approximately 40 (80 rings per chain). These results are based on the assumption that each polymer chain has two *tert*-butyl groups as chain ends. The possibility exists that the polymer chain ends are not properly capped, as hydrolysis of the boronic acid group may occur to some extent during polymerization, leading to somewhat high X_n values.

Polymer Viscometry. Since the determination of the molecular weight of these polymers is a challenge, the viscometric behavior of a solution can give insight into the macroscopic properties of the polymer. Therefore, the viscosity of PPP−OSO_3 aqueous solutions was compared to that of fully sulfonated polystyrene polyelectrolytes of different molecular weights. It was found that the specific viscosity in water of a PSS of M_w equal to 8000 was identical with that of PPP−$OPSO_3$ at a concentration of 0.07 g/dL.

It is known for classical polyelectrolytes that, in dilute solutions, a polyion will take on a rodlike shape due to electrostatic self-repulsion. At a high concentration of polymer chains, where the interchain separation becomes much smaller than the rod length, the chains are flexible. Screening of the charges by added salt will also increase the flexibility though the extent of the effect may be different. Indeed, an increase in the polymer concentration increases the specific viscosity, as illustrated in Figure 3 for PPP−$OPSO_3$ in deionized water, along with 0.001 and 0.1 M $NaNO_3$ solution.

Charged flexible polymers exhibit an increase in the reduced viscosity (η_{sp}/c) with decreasing polymer segment concentration, in contrast to the behavior of ordinary polymer solutions. It is interesting to note that PPP−$OPSO_3$ shows the same behavior in water, and to a lesser extent in a low ionic strength solution, as represented in Figure 4. When the ionic strength increases, the viscosity becomes independent of the polymer segment concentration. The sharp increase, as observed for the no salt solution, is usually interpreted in terms of the Fuoss relationship.

Table 3. Values of the Fuoss Equation Coefficients for Different Ionic Strength Solutions.

salt concn (mol/L)	*A*	*B*
0	0.483	3.86
0.001	0.317	2.75
0.1	0.27	5.55

$$\eta_{red} = A(1 + Bc^{1/2}) \quad (1)$$

This relation holds well for the salt-free solution and for the salt solution above concentrations of 0.12 mg/dL. The values calculated for *A* and *B* in the Fuoss relationship are summarized in Table 3.

While there is clearly a coefficient dependence on the ionic strength, no definite relation can be established between the value of the coefficients *A* and *B* and the salt concentration. A more detailed analysis of the viscometric behavior of PPP−$OPSO_3$ goes beyond the scope of this paper. In summary, the viscometric study showed that PPP−$OPSO_3$ behaves like a semiflexible polyion, where at low chain concentrations the chains are stiffer than at high segment concentrations. As with classical polyelectrolytes, an increase in the ionic strength of the medium leads to an independence of the reduced viscosity with polymer concentration.

UV−Visible Absorption Spectroscopy. The UV−vis spectra of PPP−$OPSO_3$ and PPBP−$OPSO_3$ synthesized at pH = 8.0, 10.0, and 12.0 were obtained in aqueous solutions in order to monitor the bathochromic shift that occurs during the formation of the *p*-phenylene linkages. The λ_{max} of the long-wavelength absorptions could also be used as a tool to indirectly monitor the degree of polymerization, as increased chain lengths result in a red-shift in the absorption at low molecular weights.

As shown in Table 1, λ_{max} of the long-wavelength absorption for PPP−$OPSO_3$ was observed between 339

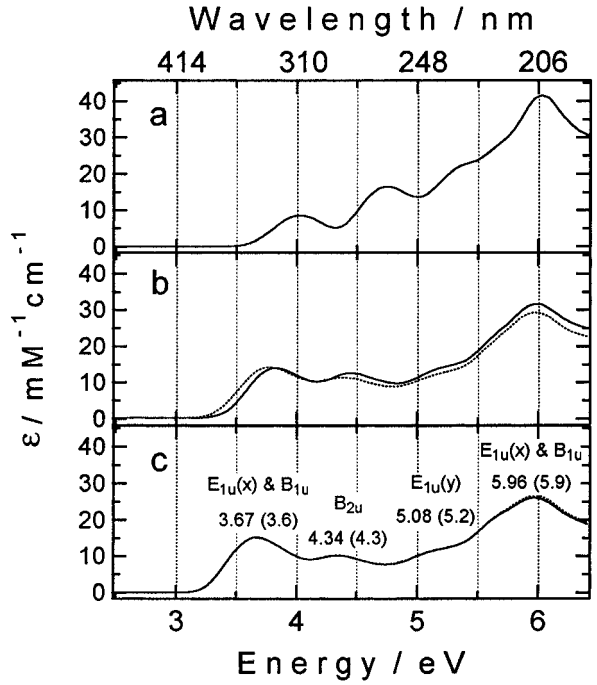

Figure 5. UV−visible absorption spectra of selected monomer, oligomer, and polymer samples in aqueous solution: (a) terphenyl model **8**; (b) (solid line) TBPPP−$OPSO_3$ sample **10a** ($X_n = 4$), (broken line) TBPPP−$OPSO_3$ oligomer **10b** ($X_n = 7.4$); (c) (solid line) PPP−$OPSO_3$ sample **1f** ($X_n = 17$), (broken line) PPP−$OPSO_3$ sample **1e** ($X_n = 17$). Abscissa scaled in units of molar absorptivity (M^{-1} cm^{-1}). For oligomer and polymer samples, concentration refers to concentration of monomer repeat unit. In panel c the spectral assignments are indicated along with the observed and calculated (in parentheses) absorption band energies.

and 342 nm at all three pH's when the water soluble Pd(0) complex was used and at pH 10.0 and 12.0 when $Pd(OAc)_2$ was employed. PPBP−$OPSO_3$ showed a bathochromic shift to 349−352 nm when the polymerization was carried out at pH 10.0 and 12.0. Comparison of these results indicates that the less substituted PPBP−$OPSO_3$ are slightly more conjugated due to the lower degree of substitution. The polymerizations were less effective at the lower pH. In fact, PPBP−$OPSO_3$ could not be isolated at pH 8.0. The diboronate ester monomer (**4**) is only slightly soluble in the aqueous buffer, precluding reaction.

More detailed UV−visible absorption spectral studies were carried out on the terphenyl model compound **8** and selected oligomer and polymer samples to examine the effect of chain length on the spectra. Absorption spectra were obtained on aqueous solutions with known oligomer or polymer concentration (expressed as repeat unit concentration), thereby allowing comparison of the absolute absorptivity of the materials. Figure 5 compares the spectra of **8** (Figure 5a), TBPP−$OPSO_3$ oligomers **10a** and **10b** (Figure 5b), and PPP−$OPSO_3$ polymers **1e** and **1f** (Figure 5c), while Table 4 lists absorption maxima and extinction coefficients. Several interesting features emerge from comparison of these spectra. First, the spectrum of **8** displays three clearly resolved bands (and one shoulder). By comparison, *p*-terphenyl features only two bands at 206 and 278 nm, which are assigned, respectively, to transitions derived from the $^1E_{1u}$ and $^1B_{1u}$ states of benzene.[18−20] Clearly the highest energy band in the spectrum of **8** (206 nm) corresponds to a transition that is derived from the $^1E_{1u}$ benzene state. Assignment of the two resolved bands at lower energy in **8** is less certain; however, it is likely that they arise from transitions derived from the $^1B_{1u}$ and $^1B_{2u}$ states of benzene.[18−20]

Oligomers **10a** and **10b** also feature three well-resolved absorption bands and one weak, poorly resolved band. The lowest energy band in both samples is shifted to lower energy relative to the lowest transition in **8**. Furthermore, the oscillator strength of the high-energy band at 6 eV (208 nm) is decreased in the oligomers relative to **8**, while that for the lowest energy transition at 3.7 eV (325 nm) is increased relative to **8**. This pattern suggests that in the oligomers oscillator strength is transferred from the high-energy band into the lowest transition. Interestingly, the two lowest energy transitions in **10b** ($X_n = 7.4$) are distinctly red-shifted compared to their position in **10a** ($X_n = 4$). Furthermore, in the longer oligomer (**10b**) the oscillator strength of the low-energy and high-energy bands is increased and decreased, respectively, compared to the shorter oligomer. The absorption changes seen on going from **8** to **10a** (or **10b**) are even more pronounced in the spectra of PPP−$OPSO_3$ samples **1e** and **1f** (Figure 5c) in which the PPP chain length is increased. Thus, the two lowest energy bands are shifted to even lower energy, and the transfer of oscillator strength from the 6 eV band into the lowest energy transition at 3.6 eV is more pronounced.

Our analysis of the absorption spectra of the oligomer and polymer samples follows the theory recently developed by Garstein and Rice (G & R),[21−24] which describes PPP oligomer and polymer excitations as being derived from the local excitations of the phenylene monomers (i.e., benzene). Their theory indicates that PPP materials should exhibit four exciton bands (three allowed and one forbidden) that are derived from the benzene excitations (listed in order of increasing energy) $E_{1u}(x)$ and B_{1u}, B_{2u}, $E_{1u}(y)$, and $E_{1u}(x)$ and B_{1u} (x is the polymer long axis). Quite interestingly, the absorption spectra of the oligomer and polymer samples studied herein are in qualitative and quantitative (see below) agreement with G & R theory. Thus, the highest energy band observed at ≈6 eV is derived from the $E_{1u}(x)$ and B_{1u} states of benzene and is expected to be long axis polarized. The lowest transition, which appears at 3.6−3.7 eV and is very sensitive to the PPP chain length, is derived from the same benzene states. Coupling of the 6 and 3.6 eV transitions is clearly indicated by the fact that, as the length of the PPP chain increases, there is a transfer of oscillator strength from the former to the latter. The relatively weaker bands at intermediate energy are derived from the B_{2u} and $E_{1u}(y)$ states, which are short axis (y) polarized and are forbidden in the monomer. Interestingly, G & R have calculated the energies of the four exciton bands to be 3.6, 4.3, 5.2, and 5.9 eV, which is in nearly quantitative agreement with the energies observed for the PPP−$OPSO_3$ samples **1e** and **1f**.

Photoluminescence Spectroscopy. All of the TBPPP−$OPSO_3$ and PPP−$OPOSO_3$ oligomers and polymers described herein display strong fluorescence in the blue-green region when excited in the near-UV. Thus, to characterize the fluorescence properties of the materials, fluorescence and fluorescence excitation spectra, as well as fluorescence quantum yields (Φ_{fl}) and fluorescence lifetimes (τ_{fl}), were acquired for selected samples in aqueous solution. Figure 6 displays representative

Table 4. Photophysical Properties of Selected Monomers, Oligomers, and Polymers[a]

	spectral assignment[b]	6	10a	10b	1e	1f
λ^{abs}/nm	$E_{1u}(x)$ and B_{1u}	206 (41.6)	208 (31.6)	208 (29.3)	208 (26.1)	208 (26.1)
(ϵ_{max}/M^{-1} cm^{-1})[c]	$E_{1u}(y)$	232 (22.0)	240 (13.8)	240 (12.3)	244 (11.0)	244 (11.0)
	B_{2u}	261 (16.4)	280 (12.6)	284 (11.4)	286 (10.2)	286 (10.2)
	$E_{1u}(x)$ and B_{1u}	308 (8.52)	324 (14.0)	330 (14.2)	338 (15.2)	338 (15.2)
λ^{fl}/nm[d]		387	411 (sh)	411 (sh)	410	410
			438	438	430 (sh)	430 (sh)
$\lambda^{fl,ex}$/nm[e]		267	275	276		291
		310	324	328	348 (sh)	347 (sh)
					363	363
Φ_{fl}[f]		0.50	0.29	0.17	0.55	0.60
τ_{fl}/ns		2.0	1.3	1.0	1.1	1.0

[a] All data for deoxygenated aqueous solution, 25 °C. [b] Spectroscopic assignments for oligomer and polymer samples following Garsten and Rice.[21−24] State assignments use symmetries of benzene excitations from which they are derived. [c] Absorption band maximum. [d] Fluorescence excitation band maximum. [e] Fluorescence emission band maximum. [f] Fluorescence quantum yield, relative to anthracene in methanol (Φ_{fl} = 0.27).

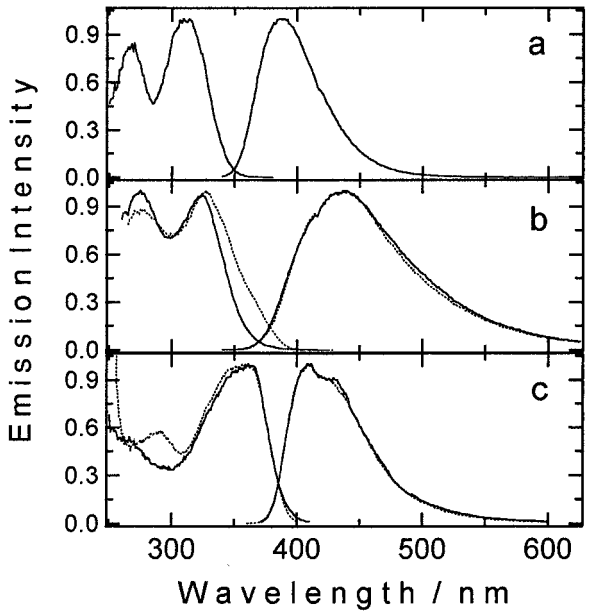

Figure 6. Fluorescence and fluorescence excitation spectra of selected monomer, oligomer, and polymer samples in aqueous solution. (a) terphenyl model **8**, fluorescence spectrum λ_{ex} = 320 nm, excitation spectrum λ_{em} = 420 nm; (b) (solid line) TBPPP−$OPSO_3$ sample **10a** (X_n = 4), fluorescence spectrum λ_{ex} = 330 nm, excitation spectrum λ_{em} = 435 nm, (broken line) TBPPP−$OPSO_3$ oligomer **10b** (X_n = 7.4), fluorescence spectrum λ_{ex} = 340 nm, excitation spectrum λ_{em} = 410 nm; (c) (solid line) PPP−$OPSO_3$ sample **1f** (X_n = 17), (broken line) PPP−$OPSO_3$ sample **1e** (X_n = 17). In each case the fluorescence spectra are at right and the fluorescence excitation spectra are at left (shorter wavelength). All spectra are normalized to maximum intensity.

fluorescence and fluorescence excitation spectra, and Φ_{fl} and τ_{fl} values are compiled in Table 4.

Model compound **8** fluoresces in the near-UV with λ_{max} = 387 nm. The fluorescence from all of the oligomer and polymer samples (**10a**, **10b**, **1e**, and **1f**) appears as a relatively broad band that is red-shifted relative to that of **8**. Furthermore, for each of the oligomer and polymer samples a shoulder is observed, either on the short- or long-wavelength side of the predominant fluorescence band maximum. Interestingly, the main fluorescence band of the longer PPP chain samples (**1e** and **1f**) is blue-shifted compared to that of the short chain PPP oligomers (**10a** and **10b**). However, it is significant that a shoulder on the short wavelength side of the fluorescence from **10a** and **10b** (Figure 6b) corresponds closely to the fluorescence band maximum of **1e** and **1f** (Figure 6c). Moreover, a shoulder on the long-wavelength side of the fluorescence band in **1e** and **1f** corresponds reasonably well with the fluorescence band maximum for **10a** and **10b**. Thus, it is possible that the short wavelength (high-energy) fluorescence band that predominates the spectra of **1e** and **1f**, and appears as a shoulder in the spectra of **10a** and **10b**, may arise from a high-energy state that is perhaps associated with the polymer end groups.

Regardless of the origin of the long-wavelength shoulder appearing in the fluorescence spectra of polymer samples **10a** and **10b**, it is important to note that these materials exhibit a very similar fluorescence band maximum compared to that of an organic-soluble dialkoxy-substituted PPP polymer with X_n > 200 synthesized by Suzuki coupling methodology.[25] Thus, the primary fluorescence band observed from **10a** and **10b** is very likely due to the $^1\pi,\pi^*$ exciton state that derives from the conjugated polymer backbone.

The fluorescence excitation spectra for model compound **8** and oligomers **10a** and **10b** closely mimic the absorption spectra. This indicates that in these systems the fluorescent state is reached with comparable efficiency, regardless of whether the excitation initially populates the band gap edge or mid-gap states. By contrast, the fluorescence excitation spectra of polymer samples **1e** and **1f** are markedly different from the absorption spectra. The most prominent excitation feature is red-shifted relative to the lowest energy absorption. Excitation spectra obtained on **1e** and **1f** at fluorescence wavelengths ranging across the entire fluorescence band (spectra not shown) do not vary significantly from those illustrated in Figure 6c. These observations suggest that the fluorescence for the highest molecular weight samples examined is dominated by states that are near the edge of the band gap. As noted above, these states may be associated with the polymer end groups, which are unknown in samples **1e** and **1f** because end-capping groups were not intentionally added during the synthesis.

Fluorescence quantum yields (Φ_{fl}) for all of the samples (Table 4) are comparatively large. Clear trends in Φ_{fl} with respect to chain length are not noticed; however, Φ_{fl} for the PPP−$OPSO_3$ polymers **1e**,**f** are somewhat larger than for the TBPPP−$OPSO_3$ end-capped oligomers **10a**,**b**. The fluorescence lifetimes (τ_{fl}) of all of the compounds are comparatively short, with the lifetimes of the oligomers and polymers being shorter than the monomer. Interestingly, the lifetimes of the PPP−$OPSO_3$ polymers **1e**,**f** are 50% shorter compared to model compound **8**, despite the fact that

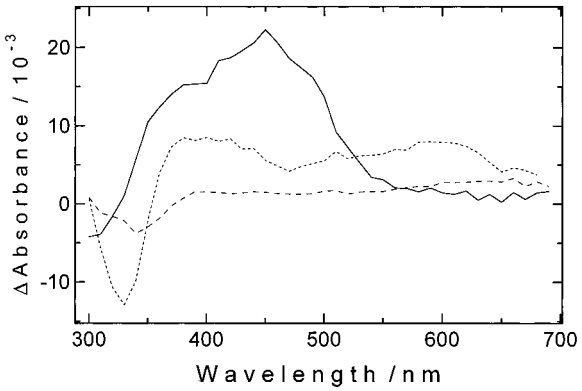

Figure 7. Transient absorption spectra of monomer, oligomer, and polymer samples in aqueous solution. (solid line) terphenyl model **8**; (dotted line) TBPPP−$OPSO_3$ sample **10a** (X_n = 4); (dashed line) PPP−$OPSO_3$ sample **1f** (X_n = 17). Principal component spectra were extracted from a global analysis of time-resolved data.

Φ_{fl} is comparable for all three samples. This observation indicates that the radiative decay rate for the polymers is larger than for the monomer. While extensive data concerning the fluorescence quantum yields and lifetimes of soluble conjugated polymers is not currently available, the photophysical parameters for the water soluble PPP polymers examined herein are consistent with the limited data for organic soluble polyphenylene-based conjugated polymers (i.e., moderate-to-large Φ_{fl} and short τ_{fl}).[26−29]

Transient Absorption Spectroscopy. Nanosecond−microsecond laser flash photolysis experiments were carried out on selected samples in order to examine the possibility that direct excitation produces long-lived triplet states. All flash photolysis was carried out on samples that had matched optical density at the laser excitation wavelength (266 nm) and with the same laser excitation energy. Thus, the transient absorption signals (ΔA) observed in the visible region for each sample are proportional to the product of the triplet state molar absorptivity (ϵ_{TT}) and the triplet yield (Φ_T),

$$A \propto \epsilon_{TT}\Phi_T \qquad (2)$$

First, flash photolysis of a solution *p*-terphenyl in methanol gives rise to a strongly absorbing transient ($\Delta A \approx 0.25$) with an absorption maximum at 450 nm (spectrum not shown). This transient is due to the triplet state, which is reported to have $\epsilon_{TT} \approx 90\,000$ M^{-1} cm^{-1} and $\Phi_T \approx 0.1$.[30] Figure 7 illustrates a comparison of the transient absorption spectra for samples **8**, **1f**, and **10a**. In each case, flash photolysis produced comparatively weakly absorbing transients having very long lifetimes (τ > 500 μs). The long lifetimes are consistent with assignment of the transients to the triplet state. The transient absorption spectrum of model compound **8** is characterized by a weak ground-state bleach (e.g., negative ΔA) for λ < 320 nm and a broad mid-visible band centered at 450 nm. This spectrum is similar to that of the terphenyl triplet state; however, the maximum ΔA observed for **8** is lower by at least 1 order of magnitude compared to that of terphenyl, which indicates that ϵ_{TT} and/or Φ_T for **8** is substantially lower compared to terphenyl. Oligomer and polymer samples **10a** and **1f** display a very weak transient that is characterized by bleaching of the lowest energy ground-state absorption band in the UV and broad absorption throughout the visible. The most obvious point is that the intensity of the ΔA signals for the oligomer and polymer samples is significantly lower than that of monomer **8**. Taken together, the available data indicate that direct excitation of the monomer produces a long-lived triplet state in modest quantum yield ($0.01 < \Phi_T < 0.1$). However, the substantially lower intensity of the transient absorption observed for the oligomer and polymer samples qualitatively implies that direct excitation of these materials produces triplet states with very low efficiency. The latter result is consistent with previous studies which indicate that triplets are formed inefficiently via direct excitation of conjugated polymers.[31]

Luminescent Self-Assembled PPP−$OPSO_3$ Films. As noted in the fluorescence studies detailed earlier, PPP−$OPSO_3$ and PPBP−$OPSO_3$ are polyanionic blue-light-emitting polymers that can be incorporated into multilayered films using layer-by-layer sequential adsorption.[32] This has been done with PPP−$OPSO_3$ for many different polycations including poly(ethylenimine), poly(allylamine), poly(vinylpyridine), poly(phenylenevinylene) precursor, and polycationic derivatized PPP. Within the context of this paper, the discussion will be limited to the films of PPP−$OPSO_3$ with poly(ethylenimine) (PEI). Details of the buildup of self-assembled films of PPP−$OPSO_3$ with other polycations and their subsequent use in blue-light-emitting devices will be discussed elsewhere.[33]

Multilayered films of PPP−$OPSO_3$ and PEI were prepared using a variety of different aqueous solution conditions on substrates of clean hydrophilic glass and patterned ITO substrates. Films made with PEI and PPP−$OPSO_3$ solution concentrations of 10^{-3} M (based on the repeat unit molecular weight) with no added salt and a pH of about 7.0 were observed to build up linearly with a relatively low absorbance per bilayer and a thickness that was too thin to be accurately measured by profilometry. However, if the solution parameters such as pH or added salt concentration are adjusted in an attempt to obtain thicker bilayers, a nonlinear buildup similar to that reported for other self-assembled structures of PEI was observed by UV−visible spectroscopy. The nonlinearity typically involves the buildup of thin films below five bilayers, followed by thicker bilayers that depend on the specific solution conditions used. For example, films made with PEI and PPP−$OPSO_3$ solution concentrations of 10^{-3} M with no added salt and a pH of about 3.5 were observed to give an estimated thickness of 8 Å/bilayer below five bilayers and 25 Å/bilayer above 5 bilayers. It should be noted that, of all the different polycations assembled with PPP−$OPSO_3$, this effect was only observed with the PEI polycation and is probably linked to the highly branched nature of PEI.

Using these latter solution parameters, 25 bilayers of PEI/PPP−$OPSO_3$ were assembled onto patterned ITO substrates with a total thickness of 540 Å. Prior to the thermal deposition of approximately 2000 Å of patterned aluminum, the films were heated under vacuum at 100 °C for 4 h to remove water. A schematic drawing of the device can be viewed in Figure 8. A typical current and light intensity versus applied voltage plot for these devices can be observed in Figure 9. As this figure shows, there is typically a small amount of leakage current for these thin films prior to the device turn-on at 7 V. Though similar devices of PPP−$OPSO_3$/PEI

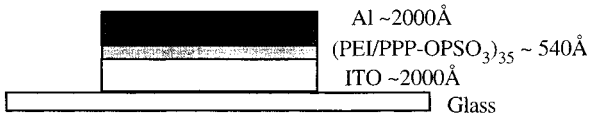

Figure 8. Schematic of EL device constructed using the PEI/PPP−$OPSO_3$ multilayer film as the emitter.

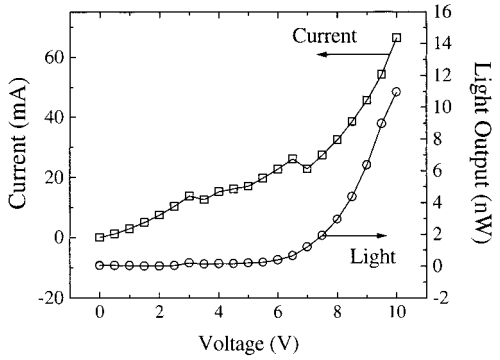

Figure 9. Voltage dependence of current and light intensity for the PEI/PPP−$OPSO_3$ multilayer film device.

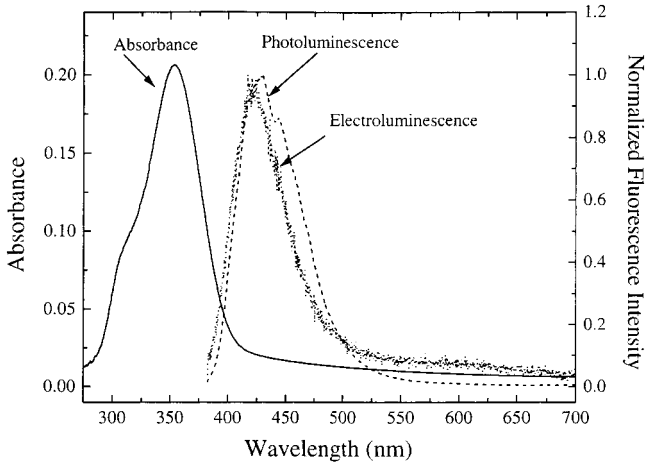

Figure 10. Absorbance, photoluminescence, and electroluminescence of a 35 bilayer self-assembled film of PPP−$OPSO_3$/PEI.

have given higher maximum light outputs of 30 nW and an estimated external quantum efficiency of up to 0.005%, the device parameters observed in Figure 9 are more typically observed. This device performance may be linked to the presence of the PEI, which is estimated to comprise about 75% of the film volume. For example, as will be discussed elsewhere,[33] when the PEI is substituted with a polycationic version of PPP under the same solution parameters, much thinner films are assembled that show no leakage current, better device reproducibility, and a higher light output of up to 100 nW. This polycationic PPP/polyanionic PPP combination also represents the first time an all conjugated LED has been made with the same electroactive species using layer-by-layer sequential adsorption. Yet, as can be observed in Figure 10, self-assembled films of PPP−$OPSO_3$ and PEI can still be used to create LEDs with a blue electroluminescence that is very similar to that of the solid-state photoluminescence. It should also be noted that the solid-state luminescence of PPP−$OPSO_3$ has been used in multilayered heterostructures of PPP−$OPSO_3$ and poly(*p*-phenylenevinylene) (PPV) to probe the level of interpenetration between spontaneously adsorbed layers via the Förster energy transfer mechanism.[33]

Experimental Section

Material Handling and Purification. 1,4-Dibromobenzene was used as received. Fresh Mg turnings were prepared by crushing Mg pellets in a mortar with a pestle before use. THF was dried over sodium/benzophenone before use. CH_2Cl_2 was dried over calcium hydride before use.

The water soluble Pd(0) catalyst (Pd[$P(C_6H_5)_2C_6H_4$-*m*-SO_3-Na]$_3$) is air sensitive, changing color from bright yellow to red immediately, thus its synthesis was carried out entirely under inert conditions. It was also found that the Pd(0) catalyst slowly changes its color under exposure to light. Therefore, the final product was transferred into a drybox and stored in a light-tight box.

The monomers were stored in a drybox and each monomer was weighed with a precision of 0.001 ± 0.0005 g for the best stoichiometric balance to obtain a high degree of polymerization. The glassware used was dried in an oven and immediately brought into the drybox in order to limit exposure to water. The reaction medium and monomers were deaerated to keep the catalyst reactivity as high as possible. The monomer-containing glassware was purged with argon for 30 min prior to solvent addition. A mixture of 70% aqueous base with 30% DMF was also deaerated for 1 h before use and transferred via cannula.

Dialysis membranes with a 3500 cutoff were used for the purification of the polymers after precipitation from acetone. For polymer samples with low molecular weights (ca. 1000 to 3000), membranes with a 500 cutoff range were used. Deionized water was used for dialysis as well as for the synthesis of the polymers. Reagent grade acetone was used for the precipitation of the products and purified by filtration before use in order to remove any particle impurities.

Characterization Methods Used. NMR spectra were obtained on Varian VXR-300 and Oxford Gemini-300 spectrometers in $CDCl_3$, DMSO-d_6, and D_2O. The polymers were only soluble in D_2O. TGA was carried out under nitrogen using a TA-2950 thermogravimetric analyzer system. For analysis, 3−14 mg samples that were initially dried within the TGA were used and the heating rate was 10 °C/min. Elemental analyses were carried out by Robertson Microlit Laboratories, Inc. Madison, NJ. Varian Cary 5E and HP-8425A diode array UV−vis spectrophotometers were used for electronic spectroscopy. The λ_{max} values before and after dialysis were measured with a resolution of 1 nm. There was no observable λ_{max} change for the $\pi-\pi^*$ absorption before and after dialysis.

Steady-state fluorescence measurements were carried out on a SPEX F-112 fluorometer. Emission and excitation scans were corrected for instrumental response using in-house generated correction factors. For emission scans, the sample optical density was approximately 0.1 at the excitation wavelength (monomer concentration ca. 2×10^{-5} M). For excitation scans, the sample optical density was less than 0.1 over the 250−400 nm region (monomer concentration ca. 2×10^{-6}). Samples were contained in degassable 1 cm × 1 cm quartz cuvettes and are reported relative to anthracene in methanol ($\Phi_{fl} = 0.27$). Fluorescence lifetimes were determined by time-correlated single photon counting on an instrument manufactured by Photochemical Research Associates. Excitation and emission wavelengths were selected by band-pass filters (excitation, Schott UG-11; emission, 400 or 450 nm interference filter). Fluorescence decay analysis was effected by the techniques of iterative reconvolution and Marquardt nonlinear least-squares analysis.

Laser flash photolysis was carried out on an instrument that has been previously described.[34] Excitation was effected by using the fourth harmonic output of a Nd:YAG laser (266 nm, 10 mJ/pulse, 10 ns fwhm). Samples were contained in a recirculating flow cell with a total volume of 100 mL to minimize possible effects due to sample photodecomposition during data acquisition. The time-resolved transient absorption data were analyzed by Factor analysis using the SPECFIT program.[35]

The GPC system combined a Waters 6000A pump, a Waters Ultrahydrogel linear mixed-bed column, and a 440 fixed wavelength detector. Viscometric measurements were carried out using a Viscotek 500Y differential viscometer maintained at 30 °C. Aqueous solutions of PPP−$OPSO_3$ in $NaNO_3$ (10^{-3} and 10^{-1} M) were made from MilliQ water by dilution from a stock solution. The polymer concentrations ranged from 10 to 200 mg/dL.

Auto-dipped multilayered films of PPP−$OPSO_3$ and PEI were assembled using a Zeiss HMS/DS-100 biological glass slide strainer. The typical automated dip cycle involved placing the substrates into the polycation solution for 15 min, rinsing with three separate static water dips of 2, 1, and 1 min each, dipping the substrates into the PPP−$OPSO_3$ solution for 15 min, and then repeating the rinsing. Separate water bins were used for rinsing of the polycation and the polyanion. The deionized water of both types of rinsing bins was changed after every five bilayers. This cycle was repeated and monitored by UV−visible spectroscopy until the desired number of bilayers were assembled onto the substrate. The substrate cleaning processes have been described elsewhere.[36]

Synthesis of 1,4-Phenylenediboronic Acid (3) and 4,4′-Biphenyldiyldiboronic Acid. 1,4-Phenylenediboronic acid and 4,4′-biphenyldiyldiboronic acid were synthesized according to the literature.[37]

Synthesis of 4,4′-Biphenyldiyldiboronic Acid 2,2′-Dimethylpropyl Ester (4). To a 100 mL round-bottom flask equipped with a Dean−Stark apparatus were added 35 mL of toluene and 25 mL of DMSO. To the solution were added 1.21 g of 4,4′-biphenyldiyldiboronic acid (0.005 mol) and 20.8 g of 2,2′-dimethyl-1,3-propanediol (Aldrich Chemical Co.) (0.20 mol). The solution was refluxed at 110 °C for 12 h and then cooled to 0 °C. The solution volume was reduced by evaporation, and 100 mL of EtOH was added. The mixture was stirred for 30 min. White crystals were collected by filtration and washed with EtOH. The product (**4**) was dried in vacuo at 60 °C for 12 h, yielding 1.85 g (97.1%): mp 249−251 °C (lit.[37] mp 250 °C); ^{1}H NMR (DMSO-d_6) δ 1.03 (s, 12H), 3.78 (s, 8H), 7.63 (d, 4H, J = 9.0 Hz), 7.88 (d, 4H, J = 9.0 Hz); ^{13}C NMR (DMSO-d_6) δ 21.91, 31.90, 76.59, 126.35, 134.31, 143.24.

Synthesis of 1,4-Dibromo-2,5-Bis(3-sulfonatopropoxy)-benzene (5). In a 500 mL round-bottom flask equipped with water condenser were added 13.8 g of 1,4-dimethoxybenzene (Aldrich Chemical Co.) (0.10 mol) and 200 mL of CCl_4 under argon. The mixture was stirred until all solids disappeared. Into the solution was added dropwise 12.4 mL of bromine (Aldrich Chemical Co.) (0.24 mol) mixed with 80 mL of CCl_4 for 30 min. The mixture was stirred for 12 h. HBr gas was collected in saturated aqueous NaOH as it evolved. A white-colored precipitate was collected by filtration and washed with cold ethanol. The filtrate was neutralized by adding aqueous 5 M K_2CO_3 with vigorous stirring until the solution turned colorless. The CCl_4 solution was separated and further product recovered by evaporation. The crude 1,4-dibromo-2,5-dimethoxybenzene was recrystallized from boiling ethanol. Subsequently, into a 500 mL round-bottom flask equipped with a water condenser were added 13.2 g of 1,4-dibromo-2,5-dimethoxybenzene and 150 mL of dry CH_2Cl_2 under argon. The mixture was stirred until all solids disappeared. Dropwise, into the solution was added 100 mL of 1.0 M boron tribromide of CH_2Cl_2. The reaction was refluxed at 45 °C for 12 h and then cooled to room temperature. The solution was slowly poured into ice−water at 0 °C and stirred vigorously for 30 min. An off-white precipitate was separated by filtration and washed with water. Pure 1,4-dibromohydroquinone was collected and dried in vacuo at 60 °C for 12 h. The product was used without further purification. Into a 500 mL round-bottom flask equipped with a water condenser were added 5.36 g of 1,4-dibromohydroquinone (0.020 mol) and 100 mL of anhydrous EtOH under argon. The mixture was stirred until all solids disappeared. In 100 mL of EtOH was dissolved 1.70 g of NaOH (0.044 mol). The NaOH in EtOH was added dropwise and stirred for 1 h, causing the yellow solution to turn orange-red. Into the solution was added 5.39 g of 1,3-propanesultone (Aldrich Chemical Co.) (0.042 mol) in 50 mL of EtOH. The reaction was vigorously stirred for 12 h and a white product precipitated from the solution. The product was collected by filtration, washed with EtOH, and recrystallized twice from water to yield 1,4-dibromo-2,5-bis(3-sulfonatopropoxy)benzene (**5**) 5.68 g (51.2%) after drying in vacuo at 100 °C for 12 h: ^{1}H NMR (D_2O) δ 2.20 (t, 4H, J = 6.9 Hz), 3.13 (qt, 4H, J = 2.4 Hz), 4.10 (d, 4H, J = 6.3 Hz), 7.21 (s, 2H); ^{13}C NMR (D_2O) δ 24.62, 48.22, 69.37, 111.36, 119.56, 149.76.

Synthesis of Tris((diphenylphosphino)benzene-*m*-sulfonic acid)palladium(0) Sodium Salt Catalyst (6). Tris-((diphenylphosphino)benzene-*m*-sulfonic acid) palladium(0) sodium salt was synthesized according to a literature procedure.[7a]

Synthesis of 2,5-Diphenyl-1,4-bis(2-sulfonatopropoxy)-benzene Sodium Salt (8). Into a 250 mL three-neck flask equipped with a mechanical stirrer were added 0.834 g of 1,4-dibromo-2,5-bis(3-sulfonatopropoxy)benzene (**5**) (1.5 mmol) and 0.366 g of phenylboronic acid (3.0 mmol) under argon. Into the mixture was transferred in a drybox 0.052 g of water soluble Pd(0) complex (3 mol %), or 0.010 g of $Pd(OAc)_2$ (Aldrich Chemical Co.) (3 mol %). The contents were purged under argon for 30 min. Subsequently, 100 mL of a 70% aqueous 0.2 M Na_2CO_3/30% DMF mixture was transferred via cannula after deaeration for 1 h. The reaction was heated at 85 °C for 12 h for the water soluble Pd(0) complex (6 h for $Pd(OAc)_2$). The mixture turned black as Pd(0) particles were liberated. The filtrate was collected and then precipitated into 500 mL of acetone to yield an off-white product that was collected by filtration, recrystallized from water, and dried in vacuo at 100 °C overnight, yielding 0.46 g (55.7%): ^{1}H NMR (D_2O) δ 1.86 (t, 4H, J = 5.1 Hz), 2.69 (q, 4H, J = 2.4 Hz), 3.36 (t, 4H, J = 6.0 Hz), 6.70 (s, 2H), 7.29−7.32 (m, 4H), 7.42−7.44 (m, 6H); ^{13}C NMR (D_2O) δ 25.56, 49.26, 68.85, 117.28, 128.77, 129.48, 130.44, 131.73, 138.36, 150.54. Anal. Calcd for $C_{24}H_{24}O_8S_2Na_2 \cdot 1.5H_2O$: C, 50.34; H, 4.65; S, 10.53; Na, 7.84; Br, 0.0. Found: C, 49.91; H, 4.68; S, 11.09; Na, 7.97, Br, 0.08.

Synthesis of PPP−$OPSO_3$ (1). Into a 100 mL three-neck flask, equipped with mechanical stirrer were added 0.834 g of 1,4-dibromo-2,5-bis(3-sulfonatopropoxy)benzene (**5**) (1.5 mmol) and 0.249 g of 1,4-phenylenediboronic acid (**3**) (1.5 mmol) under argon. Into the mixture was transferred in a drybox 0.052 g of water soluble Pd(0) complex (3 mol %), or 0.010 g of Pd-$(OAc)_2$ (3 mol %). The contents were purged under argon for 30 min, and then 100 mL of 70% aqueous buffer (pH 8.0, 10.0, or 12.0)/30% DMF mixture was transferred via cannula after deaeration for 1 h. The reaction was heated at 85−90 °C for 24 h. The reaction turned black as Pd(0) particles were liberated. The tan-violet filtrate was collected, precipitated into 1 L of acetone, and redissolved in deionized water. The polymer was dialyzed using a membrane with a 3500 cutoff for 3 days. The final product, a tan-violet polymer, was obtained after drying in vacuo at 110 °C for 24 h, yielding 0.28 g (39.5%) after dialysis: ^{1}H NMR (D_2O) δ all broad peaks 2.1, 3.0, 3.9, 7.0, 7.6; ^{13}C NMR (D_2O) δ 25.4, 48.9, 68.5 (broad), 117.0, 130.2, 137.3, 150.4. Anal. Calcd for $[C_{18}H_{18}O_8S_2Na_2 \cdot 2.5H_2O]_x$: C, 41.79; H, 4.65; S, 12.39; Na, 8.89. Found: C, 43.04; H, 4.62; S, 11.21; Na, 7.92; Br, 0.15.

Synthesis of PPBP−$OPSO_3$ (2). PPBP−$OPSO_3$ was synthesized using the same method as for PPP−$OPSO_3$ with 0.834 g of 1,4-dibromo-2,5-bis(3-sulfonatopropoxy)benzene (**5**) (1.5 mmol), 0.567 g of 4,4′-biphenyldiyldiboronic acid 2,2′-dimethylpropyl diester (**4**) (1.5 mmol), and 0.052 g of water soluble Pd(0) complex (3 mol %). Yield: 0.410 g (50.0%) after dialysis. ^{1}H NMR (D_2O): δ all broad peaks 2.1, 3.0, 3.9, 7.1, 7.6. ^{13}C NMR (D_2O) δ 25.4, 48.9, 68.1 (broad), 117.0, 126.4, 130.1, 137.4, 150.3. Anal. Calcd for $[C_{24}H_{22}O_8S_2Na_2 \cdot 5H_2O]_x$: C, 45.14; H, 3.47; S, 10.04; Na, 7.20. Found: C, 46.36; H, 4.83; S, 9.15; Na, 6.36, Br, 0.30.

Synthesis of (4-*tert*-Butylphenylboronic Acid (9). Into a 250 mL three-neck flask, equipped with mechanical stirrer was transferred 10.0 mL of (4-*tert*-butylphenyl)magnesium bromide in ether (0.1 mol equiv) via cannula under argon. Into the mixture was added drop 3.5 mL of trimethylborate (0.025 mol) in dry ether 10 mL. The reaction was stirred at room temperature for 2 h, and 100 mL of cold 2 M HCl was added.

The product was extracted with 300 mL of ether. White crystals were obtained after recrystallization from water. The final product was dried in vacuo at 60 °C for 24 h, yielding 1.48 g (41.6%) after double recrystallization: ^{1}H NMR (DMSO-d_6) δ 1.34 (s, 9H), 7.41 (d, 2H, $J = 8.1$ Hz), 7.55 (d, 2H, $J = 8.1$ Hz), 7.99 (s, 2H); ^{13}C NMR (DMSO-d_6) δ 32.04, 35.36, 125.07, 135.01, 153.43.

Synthesis of TBPPP−OPSO$_3$ (10). Into a 100 mL three-neck flask, equipped with mechanical stirrer were added 0.834 g of 1,4-dibromo-2,5-bis(3-sulfonatopropoxy)benzene (**5**) (1.5 mmol) and 0.249 g of 1,4-phenylenediboronic acid (**3**) (1.5 mmol) under argon. Into the mixture, a specified amount of (4-*tert*-butylphenyl)boronic acid was added for stoichiometric imbalance for molecular weight control. Subsequently, 0.010 g of Pd(OAc)$_2$ (3 mol %) was transferred in a drybox and the contents were purged under argon for 30 min. A 100 mL aliquot of a 70% aqueous 0.2 M Na_2CO_3/30% DMF mixture was transferred via cannula after deaeration for 1 h. The reaction was heated at 85−90 °C for 24 h. The mixture turned black as Pd(0) particles were liberated. The tan-violet filtrate was precipitated into acetone, and the product redissolved in deionized water. The polymer was dialyzed using a membrane with a 500 or 3500 cutoff for 3 days according to the expected molecular weight. The final product, tan-brown to tan-violet polymers, were obtained after drying in vacuo at 110 °C for 24 h, yielding ca. 0.25 g (35%) after dialysis: ^{1}H NMR (D_2O) δ all broad peaks 1.2, 2.1, 3.0, 4.0, 7.0, 7.6.

Acknowledgment. We gratefully acknowledge support from the Air Force Office of Scientific Research (F49620-1-0067), the National Science Foundation (Grant No. CHE-9401620), and the NSF REU program.

References and Notes

(1) For a review of this area see: Schlüter, A.-D.; Wegner, G. *Acta Polym.* **1993**, *44*, 59.
(2) Ballard, D. G. H.; Courtis, A.; Shirley, I. M.; Taylor, S. C. *Macromolecules* **1988**, *21*, 294.
(3) McKean, J. K.; Stille, J. K. *Macromolecules* **1987**, *20*, 1787.
(4) Gin, D. L.; Conticello, V. P.; Grubbs, R. H. *J. Am. Chem. Soc.* **1992**, *114*, 3167.
(5) (a) Rehahn, M.; Schlüter, A.-D.; Wegner, G.; Feast, W. J. *Polymer* **1989**, *30*, 1054. (b) Rehahn, M.; Schlüter, A.-D.; Wegner, G.; Feast, W. J. *Polymer* **1989**, *30*, 1060. (c) Rehahn, M.; Schlüter, A.-D.; Wegner, G. *Makromol. Chem.* **1990**, *191*, 1991.
(6) (a) Kim, Y. H.; Webster, O. W. *J. Am. Chem. Soc.* **1990**, *112*, 4592. (b) Kim, Y. H.; Webster, O. W. *Macromolecules* **1992**, *25*, 5561.
(7) (a) Wallow, T. I.; Novak, B. M. *Polym. Prepr. (Am. Chem. Soc., Div. Polym. Chem.)* **1991**, *32* (3), 191. (b) Wallow, T. I.; Novak, B. M. *J. Am. Chem. Soc.* **1991**, *113*, 7414.
(8) (a) Rau, I. U.; Rehahn, M. *Polym. Commun.* **1993**, *34*, 2889. (b) Rau, I. U.; Rehahn, M. *Acta Polym.* **1994**, *45*, 3. (c) Brodowski, G.; Horvath, A.; Ballauf, M.; Rehahn, M. *Macromolecules* **1996**, *29*, 6962.
(9) (a) Rulkens, R.; Schulze, M.; Wegner, G. *Makromol. Rapid Commun.* **1994**, *15*, 669. (b) Cimrova, V.; Schmidt, W.; Rulkens, R.; Schulze, M.; Meyer, W.; Neher, D. *Adv. Mater.* **1996**, *8*, 585.
(10) Grem, G.; Martin, V.; Meghdadi, F.; Paar, C.; Stampfl., J.; Tasch, S.; Leising, G. *Synth. Met.* **1995**, *71*, 2193.
(11) Child, A. D.; Reynolds, J. R. *Macromolecules* **1994**, *27*, 1975.
(12) Sundaresan, N. S.; Basak, S.; Pomerantz, M.; Reynolds, J. R. *J. Chem. Soc., Chem. Commun.* **1987**, 621.
(13) (a) Gieselman, M. B.; Reynolds, J. R. *Polym. Prepr. (Am. Chem. Soc., Div. Polym. Chem.)* **1992**, *33* (1), 931. (b) Gieselman, M. B.; Reynolds, J. R. *Polym. Prepr. (Am. Chem. Soc., Div. Polym. Chem.)* **1992**, *33* (1), 1056. (c) Gieselman, M. B.; Reynolds, J. R. *Macromolecules* **1993**, *26*, 5633.
(14) Gieselman, M. B.; Reynolds, J. R. *Macromolecules* **1992**, *25*, 4832.
(15) Wallow, T. I.; Novak, B. M. *J. Org. Chem.* **1994**, *59*, 5034.
(16) (a) Wallow, T. I.; Seery, T. A. P.; Novak, B. M. *Polym. Prepr. (Am. Chem. Soc., Div. Polym. Chem.)* **1994**, *35* (1), 710. (b) Novak, B. M.; Wallow, T. I.; Goodson, F.; Loos, K. *Polym. Prepr. (Am. Chem. Soc., Div. Polym. Chem.)* **1995**, *36* (1), 693.
(17) (a) Shacklette, L. W.; Eckhart, H.; Chance R. R.; Miller, G. G.; Ivory, G. G.; Baughman *J. Chem. Phys.* **1980**, *73* (8), 4098. (b) Bredas, J. L.; Themans, B.; Fripiat, J. G.; Andre, J. M. *Phys. Rev. B* **1984**, *29*, 6761.
(18) Thulstrup, E. W.; Spanget-Larsen, J.; Gleiter, R. *Mol. Phys.* **1979**, *37*, 1381.
(19) Bofinger, N. D.; Peacock, T. E. *J. Mol. Struct. (THEOCHEM)* **1991**, *230*, 235.
(20) Birks, J. B. *Photophysics of Aromatic Molecules*; Wiley-Interscience: New York, 1970; Chapters 1 and 3.
(21) Rice, M. J.; Gartstein, Y. N. *Phys. Rev. Lett.* **1994**, *73*, 2504.
(22) Rice, M. J.; Gartstein, Y. N. *Synth. Met.* **1995**, *73*, 183.
(23) Gartstein, Y. N.; Rice, M. J.; Conwell, E. M. *Phys. Rev. B* **1995**, *52*, 1683.
(24) Gartstein, Y. N.; Rice, M. J.; Conwell, E. M. *Phys. Rev. B* **1995**, *51*, 5546.
(25) Remmers, M.; Schulze, M.; Wegner, G. *Macromol. Rapid Commun.* **1996**, *17*, 239.
(26) Davey, A. P.; Elliott, S.; Blau, W. *J. Chem. Soc., Chem. Commun.* **1995**, 1433.
(27) Bunten, K. A.; Kaakkar, A. *Macromolecules* **1996**, *29*, 2885.
(28) Herrema, J. K.; van Hutten, P. F.; Gill, R. E.; Wildeman, J.; Wieringa, R. H.; Hadziioannou, G. *Macromolecules* **1995**, *28*, 8102.
(29) Swager, T. M.; Gil, C. J.; Wrighton, M. S. *J. Phys. Chem.* **1995**, *99*, 4886.
(30) Carmichael, I.; Hug, G. L. *J. Phys. Chem. Ref. Data* **1986**, *15*, 1.
(31) Xu, B.; Holdcroft, S. *Adv. Mater.* **1994**, *6*, 325.
(32) (a) Decher, G.; Hong, J.-D.; Schmitt, J. *Thin Solid Films* **1992**, *210/211*, 831. (b) Ferriera, M.; Fou, A. C.; Rubner, M. F. *Thin Solid Films* **1994**, *244*, 806.
(33) Baur, J. W.; Rubner, M. F.; Kim, S.; Reynolds, J. R. To be published.
(34) Wang, Y.; Schanze, K. S. *Chem. Phys.* **1993**, *176*, 305.
(35) Stultz, L. K.; Binstead, R. A.; Reynolds, M. S.; Meyer, T. J. *J. Am. Chem. Soc.* **1995**, *117*, 2520.
(36) Fou, A. C.; Onitsuka, O.; Ferreira, M.; Hsieh, B.; Rubner, M. F. *J. Appl. Phys.* **1996**, *79* (10), 7501.
(37) Coutts, I. G. C.; Goldschmid, H. R.; Musgrave, O. C. *J. Chem. Soc. C* **1970**, 488.

MA970781X